nature plants

SUPPLEMENTARY INFORMATION

https://doi.org/10.1038/s41477-019-0398-8

In the format provided by the authors and unedited.

Quantifying impacts of enhancing photosynthesis on crop yield

Alex Wu[1]*, Graeme L. Hammer[1], Al Doherty[1], Susanne von Caemmerer[2] and Graham D. Farquhar[2]

[1]ARC Centre of Excellence for Translational Photosynthesis, Centre for Crop Science, Queensland Alliance for Agriculture and Food Innovation, The University of Queensland, Brisbane, Queensland, Australia. [2]ARC Centre of Excellence for Translational Photosynthesis, Division of Plant Sciences, Research School of Biology, The Australian National University, Canberra, Australian Capital Territory, Australia. *e-mail: c.wu1@uq.edu.au

Section A: Cross-scale model detail

Overarching connections between photosynthesis and crop growth model

Given soil attributes, daily weather, crop management and crop genotype information, along with potential canopy level assimilation and transpiration demand from the diurnal canopy photosynthesis-stomatal conductance model (DCaPST), the crop growth and development models for sorghum[1] and wheat[2] can generate relevant crop attributes, such as LAI and SLN, along with transpiration supply when soil water is limiting, to connect to DCaPST for each day of the crop life cycle.

In water non-limited conditions, the estimated canopy CO_2 assimilation for a day ($A_{can,DAY}$, μmol CO_2 m^{-2} day^{-1}), is used to calculate potential daily shoot biomass growth ($BIO_{shoot,DAY}$):

$$\mathrm{BIO}_{\mathrm{shoot,DAY}} = A_{\mathrm{can,DAY}} \times \frac{44\mathrm{g/mol}}{1000000} \times B/(1 + root{:}shoot) \qquad \text{(S1)}$$

where, B is 0.4 g biomass (g CO_2)$^{-1}$ for cereal crops such as rice and maize[3] and *root*:*shoot* is the ratio of the biomass allocation between roots and above-ground shoot and its value, which varies through crop development stages, is taken from APSIM crop modules. A ratio of 1:1 means an equal amount of biomass is allocated to the shoot and roots. Under water non-limited conditions, the integration of leaf transpiration estimates also provides the daily canopy transpiration demand that influences the crop soil water balance. The interdependencies between CO_2 assimilation rate (A), stomatal conductance (g_s), transpiration rate (T) and leaf temperature (T_l) for the calculation of $A_{can,DAY}$ is described in the main text and Fig. S1, and detailed in the subsequent sections below. The figure also shows the drivers from the APSIM crop models (i.e. canopy leaf area index, specific leaf nitrogen and crop water supply) and environmental factors (i.e. radiation, temperature, vapour pressure deficit

and [CO_2]), and DCaPST output to return to the crop models (i.e. $BIO_{shoot,DAY}$ and daily crop water demand).

In water-limited conditions, daily crop transpiration ($T_{can,S,DAY}$) is limited by the amount of available soil water (SW_{avail}) above the lower limit of possible extraction (ll) in the part of the soil profile occupied by roots, combined with the rate at which roots can extract that water. In the crop model, an empirically derived constant (k_l) is defined incorporating both plant and soil factors that limit rate of water uptake[4]. $T_{can,S,DAY}$ is then calculated as:

$$T_{\mathrm{can,S,DAY}} = \sum_{i=1}^{n} k_{\mathrm{l},i}\left(SW_{\mathrm{avail},i} - ll_i\right) \quad \text{(S2)}$$

where n is the number of soil layers. Under these conditions, the crop transpiration allowable determines leaf transpiration possible throughout the day and limits the calculated value of $A_{can,DAY}$, as described in the main text. The soil evaporation component of the water balance was calculated based on the fraction of incident energy reaching the soil surface and surface wetness[5].

Canopy light (photosynthetically active radiation) absorption

Leaf area index of the canopy (LAI_{can}, m^2 leaf m^{-2} ground) is partitioned into sunlit and shaded leaf fractions and the ratio of these fractions changes depending on both solar and leaf angles[6]. Given leaf optical properties (reflection and scattering), total canopy absorbed photosynthetically active radiation ($I_{abs,can}$, μmol PAR m^{-2} s^{-1}) is estimated using the procedures set out by de Pury and Farquhar[7]:

$$I_{\mathrm{abs,can}} = (1-\rho_{\mathrm{cb}})I_{\mathrm{dir}}[1-\exp(-k'_{\mathrm{b}}LAI_{\mathrm{can}})] + (1-\rho_{\mathrm{cd}})I_{\mathrm{dif}}[1-\exp(-k'_{\mathrm{d}}LAI_{\mathrm{can}})] \quad \text{(S3)}$$

where ρ_{cb} and ρ_{cd} are the canopy-level reflection coefficients for direct and diffuse radiation, I_{dir} (J m^{-2} s^{-1}) and I_{dif} (J m^{-2} s^{-1}) are the direct and diffuse radiation, which are influenced by

solar angle and atmospheric transmission ratio as set out by Wu *et al.*[8], k'_{b} is the direct and scattered direct radiation extinction coefficient (derived from solar and leaf angles as described below) and k'_{d} is the diffuse and scattered diffuse radiation extinction coefficient. Values or calculation procedures for these coefficients are given in Table S4.

Radiation absorbed by the sunlit fraction of the canopy ($I_{\mathrm{abs,sun}}$, J m^{-2} s^{-1}) is given by the sum of direct, diffuse and scattered direct radiation components:

$$I_{\mathrm{abs,sun}} = (1-\sigma)I_{\mathrm{dir}}[1-\exp(-k_{\mathrm{b}}LAI_{\mathrm{can}})]$$
$$+(1-\rho_{\mathrm{cd}})I_{\mathrm{dif}}[1-\exp(-(k'_{\mathrm{d}}+k_{\mathrm{b}})LAI_{\mathrm{can}})]\frac{k'_{\mathrm{d}}}{k'_{\mathrm{d}}+k_{\mathrm{b}}}+$$
$$I_{\mathrm{dir}}\begin{Bmatrix}(1-\rho_{\mathrm{cb}})[1-\exp(-(k'_{\mathrm{b}}+k_{\mathrm{b}})LAI_{\mathrm{can}})]\frac{k'_{\mathrm{b}}}{k'_{\mathrm{b}}+k_{\mathrm{b}}}\\ -(1-\sigma)[1-\exp(-2k_{\mathrm{b}}LAI_{\mathrm{can}})]\frac{1}{2}\end{Bmatrix} \quad \text{(S4)}$$

where σ is the leaf-level scattering coefficient, and k_{b} is the direct radiation extinction coefficient, which is dependent on the solar elevation angle and canopy-average leaf angle. k_{b} influences the partitioning of LAI_{can} into sunlit and shaded fractions following[6] (Table S4) and the calculation procedures used here are as set out by Wu *et al.*[8].

Photosynthetically active radiation absorbed by the shaded fraction ($I_{\mathrm{abs,sh}}$, J m^{-2} s^{-1}) can be calculated as the sum of absorbed diffuse and scattered direct radiation, which can be more simply calculated as the difference between $I_{\mathrm{abs,can}}$ and $I_{\mathrm{abs,sun}}$[7]:

$$I_{\mathrm{abs,sh}} = I_{\mathrm{abs,can}} - I_{\mathrm{abs,sun}} \quad \text{(S5)}$$

Dependence of leaf photosynthesis parameters (V_{cmax25}, J_{max25}, V_{pmax25} and g_{m25}) on specific leaf nitrogen

Canopy level values of these parameters were calculated according to de Pury and Farquhar[7]:

$$P_{\mathrm{can25}} = LAI_{\mathrm{can}}\chi_{\mathrm{P}}(N_{\mathrm{o}} - N_{\mathrm{b}})\frac{[1-\exp(-k_{\mathrm{n}})]}{k_{\mathrm{n}}} \quad \text{(S6)}$$

where P_{can25} is the value of the parameter in question at 25ºC for the whole canopy, χ_{P} is the slope of parameter to specific leaf nitrogen (SLN) take away N_{b} (specific leaf nitrogen below which V_{camx25}, J_{max25},V_{pmax25} and g_{m25} are zero). The coefficient of N allocation in the canopy (k_{n}) is derived from canopy nitrogen profile used in the APSIM crop models[8]:

$$k_{\mathrm{n}} = -2\ln\left(\frac{N_{\mathrm{av}}-N_{\mathrm{b}}}{N_{\mathrm{o}}-N_{\mathrm{b}}}\right) \quad \text{(S7)}$$

where N_{av} is the canopy-average SLN (in units of mmol N m^{-2}, converted from g N m^{-2} by multiplying by 1000/14), N_{o} is the SLN at the top of the canopy.

Partitioning the parameters to sunlit and shaded fractions is achieved following de Pury and Farquhar[7]. Parameter for the sunlit fraction (P_{sun25}) at 25°C is given by:

$$P_{\mathrm{sun25}} = LAI_{\mathrm{can}}\chi_{\mathrm{P}}(N_{\mathrm{o}} - N_{\mathrm{b}}) \times \frac{[1-\exp(-k_{\mathrm{n}}-k_{\mathrm{b}}LAI_{\mathrm{can}})]}{k_{\mathrm{n}}+k_{\mathrm{b}}LAI_{\mathrm{can}}} \quad \text{(S8)}$$

and that for the shaded fraction (P_{sh25}) by the difference between the whole canopy and the sunlit fraction:

$$P_{\mathrm{sh25}} = P_{\mathrm{can25}} - P_{\mathrm{sun25}} \quad \text{(S9)}$$

For g_{m25} calculation, the current model assumes a negligible k_{n}.

Temperature response of photosynthesis parameters

Exponential and curvilinear response functions (equations S10 and S11)[9,10] produce responses that follow closely with the observed temperature response of photosynthesis parameters. Equation (S11) was used to model the response of J_{max} and g_{m} both having an apparent peak (Fig. S2); the rest of the photosynthesis parameters were modelled with equation (S10). Fitting of the equations to published data is given in Fig. S2, with the fitted parameter values and source given in Table S1. To reflect the higher temperature optimum of

C_4 photosynthesis, the optimum and maximum temperatures of J_{max} and g_m are set at higher values compared to C_3 (Table S1).

The two response functions are:

$$P(T) = P_{25} e^{E_a((T+273)-297.15)/(298.15R(T+273))} \quad \text{(S10)}$$

where P_{25} is the modelled parameter value at 25°C, E_a (J mol^{-1}) is parameter specific constant, R is 8.314 J mol^{-1} K^{-1} and the curvilinear response function:

$$P(T) = P_{25} \left(\frac{2(T-T_{\min})^{\alpha}(T_{\text{opt}}-T_{\min})^{\alpha} - (T-T_{\min})^{2\alpha}}{(T_{\text{opt}}-T_{\min})^{2\alpha}} \right)^{\beta} \Big/ c_{\text{norm}} \quad \text{(S11)}$$

where $\alpha = \ln(2)/[\ln((T_{max} - T_{min})/(T_{opt} - T_{min}))]$, $\beta = 1$, c_{norm} is a normalising constant, and T_{min}, T_{opt} and T_{max} defines the temperature below which $f(T) = 0$, the temperature at the maximum value of $f(T)$, and the temperature above which $f(T) = 0$, respectively.

CO_2 diffusion to the site of Rubisco carboxylation

Air CO_2 (C_a, μbar) has to diffuse across several components before reaching the carboxylation site of Rubisco inside leaves for photosynthesis. In C_3 leaves, the leaf boundary layer, stomata and mesophyll are the key components[11]; in C_4 leaves, there is an additional bundle-sheath component[12]. Drawdown of C_a across these components depend on their conductance to CO_2 and the photosynthetic rate (A, μmol CO_2 m^{-2} s^{-1}) according to Fick's law of diffusion with the effect of a ternary system of the gases (water vapour, CO_2 and air)[13]:

$$C_\varepsilon = C_a - \frac{TC_a}{g_t + \frac{T}{2}} - \frac{A}{g_t + \frac{T}{2}} - \frac{A}{g_m} \quad \text{(S12)}$$

where the subscript "ε" can be "c" or "m" to denote the chloroplastic or mesophyll CO_2 partial pressure in the case of C_3 and C_4 photosynthesis, respectively. Leaf conductance combining the boundary layer and stomatal conductance for CO_2 (g_t) is given by $1/g_t = 1/g_b + 1/g_s$ and g_m is the mesophyll conductance for CO_2. Transpiration rate (T, mol m^{-2} s^{-1}, but

mm/hr in Fig. 2), or efflux of water vapour, affects the influx of CO_2 as molecules collide and so CO_2 drawdown across the leaf conductance is influenced by T[13]. The effect of the binary system of the gases is a slightly greater stomatal conductance and crop water use over the life cycle. An earlier version of DCaPST without such effect over-predicted crop yield at low yielding levels as "water saving" in the early season resulted in slightly higher simulated yield.

Units for leaf boundary layer and stomatal conductance are mol m^{-2} s^{-1}, consistent with units for resistance (s m^{-1}), which can be obtained by multiplying the inverse of conductance (mol m^{-2} s^{-1} bar^{-1}) by a conversion factor consisting of molar density of air (ρ_{air}, mol m^{-3}) and air pressure (ATM)[14]:

$$r_s(\text{s m}^{-1}) = \frac{1}{g_s(\text{mol m}^{-2}\text{s}^{-1})} \times \rho_{air}(\text{mol m}^{-3}) \times ATM \quad \text{(S13)}$$

where ρ_{air} is calculated using the ideal gas law and is dependent on air temperature (T_a, °C) and ATM:

$$\rho_{air} = ATM \times 100000/\left(R_{air} \times (T_a + 273)\right) \quad \text{(S14)}$$

where the 100000 is to convert ATM (taken as 1.01) from bar to Pascal, R_{air} is the specific gas constant for dry air (= 8.31 J mol^{-1} K^{-1}).

Leaf boundary layer conductance for CO_2 (g_b, m s^{-1}) is influenced by leaf width (w_l, m) and wind speed (u, m s^{-1}), which are first used to calculate leaf boundary layer resistance to heat (r_{bh}, s m^{-1})[14]:

$$r_{bh} = 100\sqrt{w_l/u} \quad \text{(S15)}$$

the factor of 100 is not unitless and this equation gives the combined value of r_{bh} for the upper and lower sides of the leaf.

From this, leaf boundary layer resistance (r_{bw}, s m^{-1}) to water vapour is calculated:

$$r_{bw} = 0.93 \times r_{bh} \quad \text{(S16)}$$

and leaf boundary layer conductance for CO_2 (g_b, m s^{-1}) is related to r_{bw} by:

$$g_b = 1/(1.37 r_{bw}) \quad \text{(S17)}$$

where 1.37 is the factor accounting for the slower diffusion of CO_2 across the leaf boundary layer compared to water vapour. In air, this is normally 1.6, but the 1.37 incorporates the non-diffusive portion of the boundary layer transfer as discussed by McPherson and Slatyer[15].

However, wind speed generally decreases with canopy depth and has been modelled with an exponential decay function[16]:

$$u = u_0 exp(-k_u L) \quad \text{(S18)}$$

where u_0 is the wind speed just above the canopy, k_u is canopy wind speed profile coefficient and L is depth from top of the canopy in term of leaf area index.

In order to estimate g_b for the sunlit and shade leaf fractions, firstly, r_{bh} is inverted to g_{bh}, u substituted with equation (S18), and integrated with respect to canopy leaf area index (LAI_{can}, m^2 leaf m^{-2} ground) to take into account the variable wind speed profile in the canopy partition to the sunlit and shaded leaf fractions[17]:

$$g_{bh,can} = 0.01\sqrt{u_0/w}\,[1 - exp(-0.5 k_u LAI_{can})]/0.5 k_u \quad \text{(S19)}$$

$$g_{bh,sun} = 0.01\sqrt{u_0/w}\,[1 - exp(-(0.5 k_u + k_b) LAI_{can})]/(0.5 k_u + k_b) \quad \text{(S20)}$$

$$g_{bh,sh} = g_{bh,can} - g_{bh,sun} \quad \text{(S21)}$$

where k_b is the light extinction coefficient of solar radiation. Then, g_{bh} values were used to obtain g_b (equations S16 and S17), which is converted to units of mol m^{-2} s^{-1} using equation (S13).

Analytical solution of the combined photosynthesis and CO_2 diffusion models

CO_2 assimilation and chloroplastic CO_2 partial pressure are interdependent, but can be solved analytically. A generalised equation derived from combining the C_3 and C_4 photosynthesis models with CO_2 diffusion models (equation S12) is used to calculate the Rubisco- (A_c, μmol CO_2 m^{-2} s^{-1}) and electron-transport- (A_j, μmol CO_2 m^{-2} s^{-1}) limited assimilation rates:

$$A_\xi = \frac{\left\{\left((p-qA_\xi)+\frac{\left[\left((p-qA_\xi)x_4+x_5\right)-A_\xi-R_\mathrm{m}\right]x_6}{g_\mathrm{bs}}\right)-\gamma^*\left(\frac{\alpha}{0.047g_{bs}}A_\xi x_7+O_\varepsilon\right)\right\}x_1}{\left((p-qA_\xi)+\frac{\left[\left((p-qA_\xi)x_4+x_5\right)-A_\xi-R_\mathrm{m}\right]x_6}{g_\mathrm{bs}}\right)+x_2\left(\frac{\alpha}{0.047g_{bs}}A_\xi x_7+O_\varepsilon\right)+x_3} - R_\mathrm{d} \qquad \text{(S22)}$$

where x_1–x_7 are lumped coefficients given in Table S2, a and u are lumped coefficients that depends on the CO_2 diffusion model used (Table S3), $\gamma^* = 0.5/S_{c/o} = 0.5/(K_o/K_c * V_{cmax}/V_{omax})$, O is the oxygen partial pressure at the site of Rubisco carboxylation and is usually taken as 210000 μbar where the subscript "ε" can be "c" or "m" to denote the chloroplastic or mesophyll CO_2 partial pressure in the case of C_3 and C_4 photosynthesis, respectively

The relationship between electron transport rate and the level of absorbed photosynthetically active radiation is[12,18]:

$$\theta J^2 - J(I_2 + J_{max}) + I_2 J_{max} = 0 \qquad \text{(S23)}$$

where θ is an empirical curvature factor and the value of 0.7 is used [12], I_2 is the useful light absorbed by PSII. I_2 is related to absorbed PAR (equations S4 and S5) by de Pury and Farquhar[7]:

$$I_2 = \frac{1-f}{2} I_{\mathrm{abs,sun}} \qquad \text{(S24)}$$

where f is a spectral correction factor.

The combined photosynthesis and CO_2 diffusion models (equation S22) are solved analytically:

$$A = \left(-\sqrt{a^2 - 4b} - a\right)/2d \quad \text{(S25)}$$

where *a*, *b*, *c* and *d* are:

$$a = -pg_{bs} - px_4x_6 - \frac{\alpha}{0.047g_{bs}} g_{bs}x_2x_7R_d - \frac{\alpha}{0.047g_{bs}} g_{bs}x_1x_7\gamma_* + qg_{bs}R_d - qg_{bs}x_1 - g_{bs}O_\varepsilon x_2 - g_{bs}x_3 + x_6R_m + qx_4x_6R_d + x_6R_d - qx_1x_4x_6 - x_1x_6 - x_5x_6 \quad \text{(S26)}$$

$$b = -d(pg_{bs}R_d - pg_{bs}x_1 + px_4x_6R_d - px_1x_4x_6 + g_{bs}x_2O_\varepsilon R_d + g_{bs}x_3R_d + g_{bs}x_1\gamma_*O_\varepsilon - x_6R_mR_d + x_1x_6R_m + x_5x_6R_d - x_1x_5x_6) \quad \text{(S27)}$$

$$d = -\frac{\alpha}{0.047g_{bs}} g_{bs}x_2x_7 + qg_{bs} + qx_4x_6 + x_6 \quad \text{(S28)}$$

In the case of the C_4 photosynthesis model, C'_m (Table S2) is solved with the following iterative procedure. Firstly, the PEP-saturated rate of assimilation (A_c) was calculated with the analytical equation using an estimated C'_m (starting value of 160 μbar). The calculated *A* was used to calculate C_m ($C_m = C_i - A/g_m$), which is compared with C'_m, and then exiting the iteration when the absolute difference between C'_m and C_m is less than a specified tolerance value. See below for a simplified approach if leaf temperature is also to be solved.

Solving for stomatal conductance when water supply is non-limiting

For C_3, calculations of C_c and *A* were interdependent and so an analytical solution was invoked (equation S25). In the case of the more complex C_4 model, an additional iteration loop is implemented to solve for mesophyll CO_2 partial pressure (C_m, μbar) (equation S25 and Table S3) for the analytical solution to give *A* and the bundle sheath CO_2 partial pressure (C_s). To simulate potential *A* for the sunlit and shade leaf fractions, the ratio of intercellular to air CO_2 partial pressure (C_i/C_a) is taken as a constant despite changes in *A*, [CO_2] and light

intensity[19]. Once *A* values for the two leaf fractions were calculated, their stomatal conductance (g_s, mol m^{-2} s^{-1}) was determined by (rearranging) equation (S12) (without the mesophyll component):

$$C_i = C_i/C_a \times C_a = C_a - \frac{TC_a}{g_t + \frac{T}{2}} - \frac{A}{g_t + \frac{T}{2}} \quad \text{(S29)}$$

where *T* is transpiration rate and g_s is given by $1/g_s = 1/g_t - 1/g_b$. *T* is given by[13]:

$$T = \frac{g_{tw}(W_l - W_a)}{1000 - \frac{W_l + W_a}{2}} \quad \text{(S30)}$$

where g_{tw} is the leaf conductance for water vapour, which is given by:

$$\frac{1}{g_{tw}} = \frac{1}{g_{bw}} + \frac{1}{g_{sw}} = \frac{1}{1.37 g_b} + \frac{1}{1.6 g_s} \quad \text{(S31)}$$

where the factors account for the faster diffusion of water vapour through the boundary layer and stomata. Equation (S31) can also be written in resistance terms:

$$r_{tw} = r_{bw} + r_{sw} = \frac{r_b}{1.37} + \frac{r_s}{1.6} \quad \text{(S32)}$$

Equations (S29) and (S30) are combined and solved giving g_s:

$$g_s = 2d/\left(\sqrt{a^2 - 4b} - a\right) \quad \text{(S33)}$$

where *a*, *b*, *c* and *d* are:

$$a = \frac{1.37}{g_b} A + \frac{1.6}{g_b} A + 1.37 \times 1.6 \frac{(W_l - W_a)(C_a + C_i)/2}{1000 - (W_l + W_a)/2} - 1.37(C_a - C_i) \quad \text{(S34)}$$

$$b = d\left(1.6\left(\frac{1}{g_b}\right)^2 A + \frac{1.37 \times 1.6}{g_b} \frac{(W_l - W_a)(C_a + C_i)/2}{C_a - C_i} - \frac{1.6}{g_b}(C_a - C_i)\right) \quad \text{(S35)}$$

$$d = 1.37A \quad \text{(S36)}$$

where W_l and W_a are the water vapour mole fractions inside the leaf and in the outside air, respectively.

Water vapour mole fraction (mmol H_2O (mol air)$^{-1}$) is calculated by:

$$W = \frac{0.61365e^{\frac{17.502T_\xi}{240.97+T_\xi}}}{100ATM} \times 1000 \quad \text{(S37)}$$

where T_ξ is leaf or dew-point temperature in °C, *ATM* is taken as 1.01325 bar and the factor of 100 is to convert *ATM* to units of kPa.

The values of g_s influence transpiration (T) and leaf temperature (T_l), which generates further influences on A (Fig. S1). This interdependency was captured with an iterative procedure. Firstly, A was calculated with the analytical solution (equation S25) using an estimated T_l' (in the case of C_4, iteration is required to optimise C_m to solve for A as described above), then g_s was calculated with equation (S33), which was converted to r_s (equation S13) and used to estimate T with the Penman-Monteith Combination equation (S38), derived by combining a leaf energy balance approach with a saturation heat equation[14], and T_l with the saturation heat equation (S42), which was then compared to T_l', and then exiting the iteration when the absolute difference between T_l* and T_l was less than a specified tolerance value. In the case of C_4, both T_l and C_m are compared to T_l' and C_m' at the same time and iterated simultaneously, which is more efficient and still effective in solving for their values.

Leaf transpiration and energy balance

Leaf transpiration (T, kg H_2O m^{-2} s^{-1}), or latent heat loss (λT, W m^{-2}), was estimated with the Penman-Monteith Combination equation[14], which combines a leaf energy balance (absorbed short-wave radiation, outgoing thermal radiation, sensible heat and outgoing latent heat) and saturation heat equation:

$$\lambda T = \frac{sR_n + VPD_{l-a}\rho c_p / r_{bh}}{s + \gamma(r_{sw} + r_{bw})/r_{bh}} \quad \text{(S38)}$$

where λ is the latent heat of vaporisation of H_2O (2447000 J kg^{-1} H_2O[20]), net absorbed radiation (R_n) is the absorbed short-wave radiation minus outgoing thermal radiation, γ is the

psychrometric constant (0.066 kPa °C[20]). *s* can be simply and accurately calculated as the difference between the saturated air vapour pressure (*SVP*a, kPa) at T_a + 1 and T_a[14] and the resistance symbols (r_{sw}, r_{bw}) are stomatal and leaf boundary layer resistance to water vapour and r_{bh} is the leaf boundary layer resistance to heat as defined above.

The terms R_n and $VPD_{l\text{-}a}$ are influenced by leaf temperature, but the iteration loop described above for solving the combined photosynthesis and CO_2 diffusion models would also solve for the correct R_n and $VPD_{l\text{-}a}$.

Net absorbed radiation (R_n, W m^{-2}) was calculated as absorbed short-wave radiation ($R_{n,s}$, W m^{-2}) less outgoing thermal radiation due to the temperature differential between leaf and the surrounding air[14]:

$$R_n = R_{n,s} - 2\sigma((T_l + 273)^4 - (T_a + 273)^4) \quad \text{(S39)}$$

where σ is the Stefan-Boltzmann constant and has the value $5.668 \cdot 10^{-8}$ W m^{-2} K^{-4}, and T_l and T_a are leaf and air temperatures, respectively. The factor of 2 reflect the fact that both sides of the leaf emit thermal radiation.

Leaf-to-air vapour pressure difference ($VPD_{l\text{-}a}$, kPa) was calculated by the difference between *SVP* at T_l and *SVP* at dew point temperature (taken as T_{a_min}):

$$VPD_{l-a} = SVP_l - SVP_d \quad \text{(S40)}$$

where *SVP* at a temperature (e.g. air temperature) given by:

$$SVP = 0.61365e^{\frac{17.502T_a}{240.97+T_a}} \quad \text{(S41)}$$

Absorbed radiation (R_{abs}, W m^{-2}) is categorised as photosynthetic active radiation (PAR; 400–700 nm) and near-infrared radiation (NIR; > 700 nm). At the Earth's surface, half of the

incident solar radiation energy is assumed to be in the PAR and the other half in the NIR waveband[16]. Equations (S3)–(S5) are applied separately to PAR and NIR because they have different σ, ρ_{cb}, ρ_{cd}, k'_b, k'_d (Table S4). The sum of absorbed PAR and NIR gives R_{abs} for equation (S39).

The saturation heat equation[14] is rearranged to calculate the leaf-to-air temperature differential (ΔT):

$$\Delta T = T_l - T_a = \frac{\gamma(r_{tw})R_n/\rho c_p - VPD_{l-a}}{s+\gamma(r_{tw})} \quad \text{(S42)}$$

where r_{tw} is the leaf resistance to water vapour and the other symbols are those described for equation (S38). r_{tw} is given by the inverse of g_{tw} (equation S31).

Solving for stomatal conductance when water supply is limited

Under water-limited condition, transpiration influences stomatal conductance and leaf energy balance (Fig. S1). The Penman-Monteith Combination (equation S38) can be used inversely to calculate g_s (equations S43) and then T_l from equation (S42).

Rearranging the Penman-Monteith Combination (equation S38) for leaf resistance to water:

$$r_{tw} = \frac{(sR_n + VPD_{l-a}\rho c_p/r_{bh} - s\lambda E)r_{bh}}{\lambda E \times \gamma} \quad \text{(S43)}$$

where r_{tw}, the inverse of g_{tw}, is related to g_s by equation (S31), and other symbols have been described above.

Figures

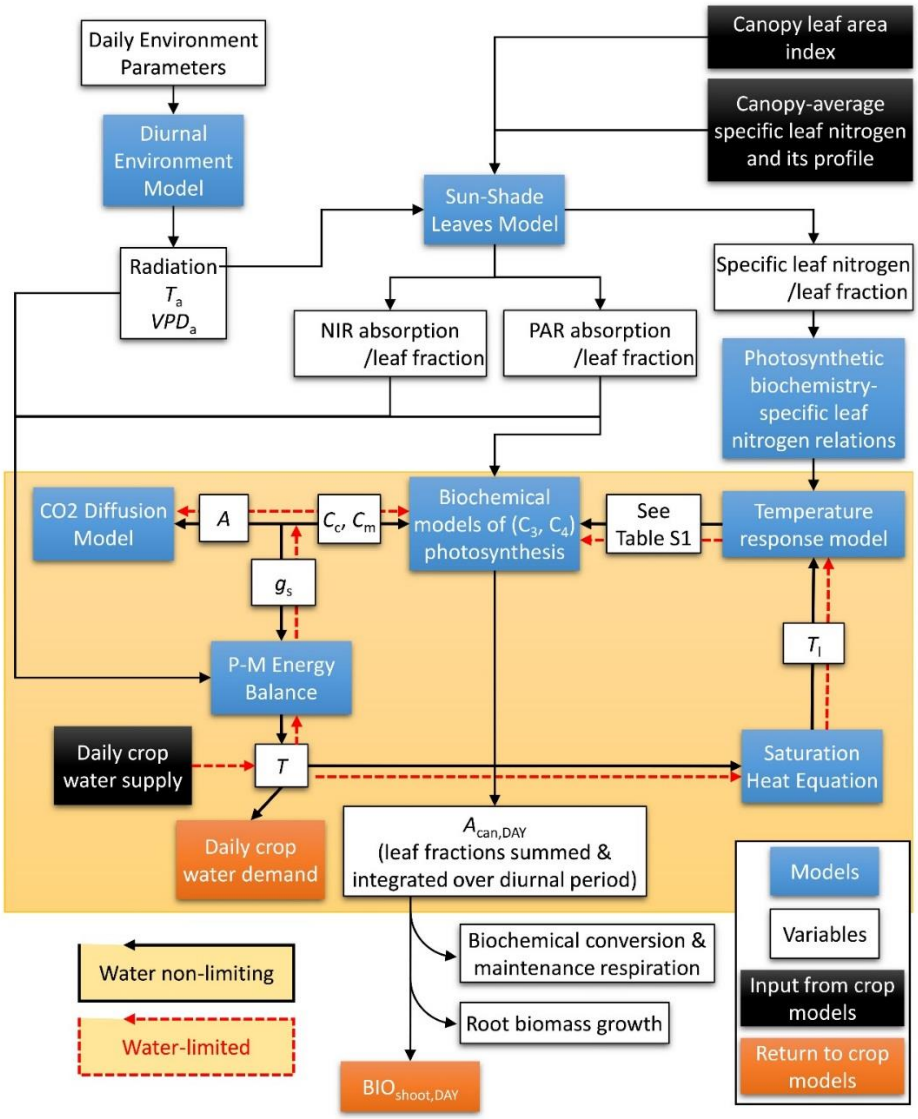

Fig. S1. A schematic of the diurnal canopy photosynthesis-stomatal conductance module and its connection with the APSIM sorghum and wheat crop models. The components encompassed by the orange-shaded background show the interdependencies between CO_2 assimilation rate (A), stomatal conductance (g_s), transpiration rate (T) and leaf temperature (T_l) for the calculation of $A_{can,DAY}$. Note the different directions in the arrows associated with g_s under water non-limiting and water-limited situations, reflecting the drivers operating in the different situations.

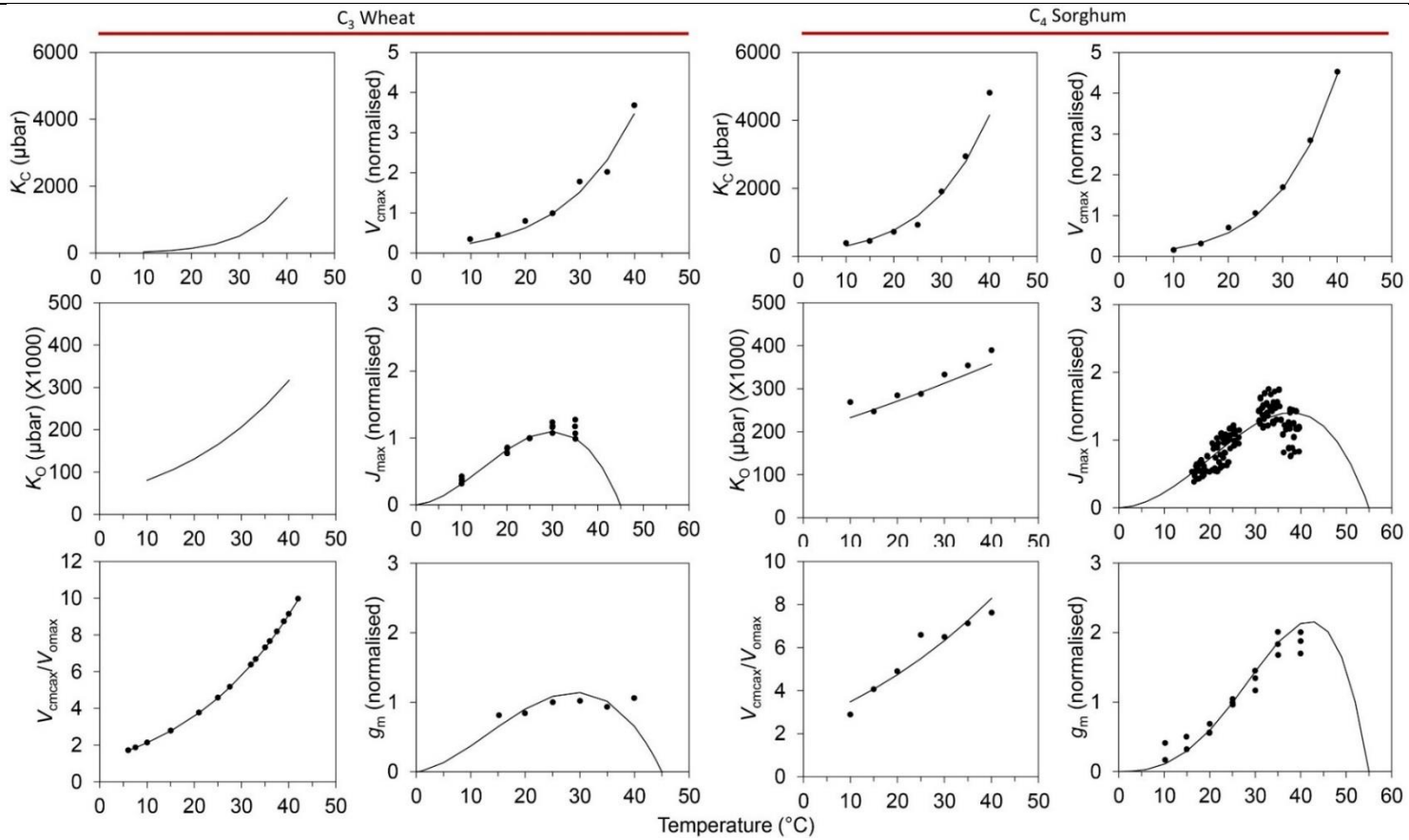

Fig. S2. Temperature response of the parameters of the C_3 and C_4 photosynthesis models. Data showing an exponential trend are fitted with equation (S10) and when there is an apparent peak, equation (S11) is used. Raw data sources and fitted parameters are given in Table S1. C_3 K_C and K_O were simulated using Rubisco kinetic constants from Silva-Pérez *et al*.[21].

Tables

Table S1. Fitted parameter values of the temperature response functions (equations S10 and S11).

		C3							C4					
	Units	Raw data source	P_{25}	E_a					Raw data source	P_{25}	E_a			
K_c	µbar	Derived from the effective Rubisco Michaelis-Menten constant for CO_2[21]	273.42	93720					[9]	1210	64200			
K_o	µbar	Derived from the effective Rubisco Michaelis-Menten constant for CO_2[21]	165820	33600					[9]	292000	10500			
V_{cmax}	µmol CO_2 m^{-1} s^{-1}	[22]	[a]	65330					[9]	[a]	78000			
V_{cmax} /V_{omax}	-	Calculated from Γ^*[23]	4.60	35713					Calculated from $S_{c/o}$[9]	5.51	21270			
K_p	µbar		-	-	-	-	-		[9]	75	36300			
V_{pmax}	µmol CO_2 m^{-1} s^{-1}		[a]	-	-	-	-		Fitted using equation (S10) to V_{pmax}[9]	-[a]	57040			
R_d	µmol CO_2 m^{-1} s^{-1}	[22]	-	46390					[22]	-	46390			
			P_{25}	T_{min}	T_{opt}	T_{max}	c_{norm}			P_{25}	T_{min}	T_{opt}	T_{max}	c_{norm}
J_{max}	µmol CO_2 m^{-1} s^{-1}	[24]	[a]	0	30.0	42.0	0.9110		[25]	[a]	0	37.86	55.0	0.7112
g_m	mol CO_2 m^{-2} s^{-1} bar^{-1}	[26]	[a]	0	29.2	45.0	0.8758		[27]	[a]	0	42.0	55.0	0.4628

Symbols: P_{25} is the modelled parameter value at 25°C, E_a is a fitted constant, T_{min}, T_{opt} and T_{max} are fitted minimum, optimum and maximum temperature of the curvilinear function, which is scaled by a constant c_{norm}. The subscript "a" indicates calculated variable using equations (S6)–(S9), where the equation parameter values are given in Table S6.

Table S2. Lumped coefficients for the Rubisco (A_c) and electron-transport limited (A_j) rate of the C_3 and C_4 photosynthesis models combined with the CO_2 diffusion model.

	x_1	x_2	x_3	x_4	x_5	x_6	x_7
Lumped coefficients for the C_3 model							
A_c	V_{cmax}	0	$K_c(1+O_c/K_o)$	0	0	0	0
A_j	$J/4$	$2\gamma_*$	0	0	0	0	0
Lumped coefficients for the C_4 model							
Ac (PEP-saturated rate)	V_{cmax}	K_c/K_o	K_c	$V_{pmax}/(C'_m + K_p)$	0	1	1
Ac (PEP-regeneration-limited rate)				0	V_{pr}	1	1
Aj	$(1-x)J_t/3$	$7/3\gamma_*$	0	0	xJ_t/φ	0	0

Symbols: J_t is the total electron transport rate generated by the mesophyll and bundle sheath, C'_m is estimated mesophyll CO_2 partial pressure, which needs to be solved iteratively, V_{pr} is the PEP-regeneration rate, φ is the number of ATP required to operate the carbon concentrating mechanism in the mesophyll and x is the fraction of ATP required in the mesophyll, which is related to $\varphi/(3 + \varphi)$ where 3 is proportional to the ATP requirement of the C_3 cycle in the bundle sheath.

Table S3. Lumped coefficients for the constant C_i/C_a approach and the full CO_2 diffusion modelling approach (equation S12).

	p	q
Constant C_i/C_a model	$C_i/C_a \times C_a$	$\frac{1}{g_m}$
Full CO_2 diffusion model	$C_a - \frac{TC_a}{g_t + T/2}$	$\frac{1}{g_t + T/2} + \frac{1}{g_m}$

Table S4. Values of leaf optical property parameters for photosynthetically active radiation (PAR)[7] and near-infrared radiation (NIR)[16].

	PAR	NIR
σ	0.15	0.8
ρ_h	$\frac{1-(1-\sigma)^{1/2}}{1+(1-\sigma)^{1/2}}$	
ρ_{cb}	$1-\exp[2\rho_h k_b/(1+k_b)]$	
ρ_{cd}	0.036	0.389
k_b	$G/\sin(\alpha)$	
k'_b	$k_b(1-\sigma)^{0.5}$	
k_d	0.78	0.8
k'_d	$k_d(1-\sigma)^{0.5}$	

Symbols: σ is the leaf-level scattering coefficient, ρ_h is the reflection coefficient of a canopy with horizontal leaves, ρ_{cb} is the canopy-level reflection coefficient for direct radiation, ρ_{cd} is the canopy-level reflection coefficient for diffuse radiation, k_b is the direct radiation extinction coefficient, k'_b is the direct and scattered direct radiation extinction coefficient, G is the shadow projection coefficient, α is solar elevation angle, k_d is the diffuse radiation extinction coefficient, k'_b is the diffuse and scattered diffuse radiation extinction coefficient.

Table S5. Environmental parameters used for simulating diurnal C_3 and C_4 canopy photosynthesis in Fig. 2.

Symbol	Description	Units	C_3 wheat value	C_4 sorghum value
Lat	Latitude	°	-27.18	-27.18
DAY	Day of year	-	288 (Spring)	12 (Summer)
RATIO	Daily atmospheric transmission ratio	-	0.75 (clear sky)	0.75 (clear sky)
T_{a_max}	Daily maximum air temperature	°C	27.6[a]	32[a]
T_{a_min}	Daily minimum air temperature	°C	12.6[a]	18.5[a]
u	Wind speed	m s^{-1}	1.5[b]	1.5[b]

[a], http://www.weatherzone.com.au/climate/station.jsp?lt=site&lc=41023

[b], Wind speed of 1.5 m s^{-1} is a good average for the Australian sorghum/wheat belt[28].

Table S6. Generic C_3 wheat and C_4 sorghum DCaPST photosynthesis and canopy parameterisation. Refer to Wu *et al.*[8] for a complete list of the default values of parameters required to run DCaPST.

Symbol	Description	Units	C_3 wheat	C_4 sorghum (short)	C_4 sorghum (tall)[e]
χ_{Vc}	Slope of linear relationship between V_{cmax} per leaf area at 25°C and specific leaf nitrogen	mmol CO_2 mol^{-1} N s^{-1}	1.1[a]	0.18[h]	0.47[b]
χ_J	Slope of linear relationship between J_{max} per leaf area at 25°C and specific leaf nitrogen	mmol CO_2 mol^{-1} N s^{-1}	1.85[a]	1.08[h]	2.70[b]
χ_{Vp}	Slope of linear relationship between V_{pmax} per leaf area at 25°C and specific leaf nitrogen	mmol CO_2 mol^{-1} N s^{-1}	NA	0.62[h]	1.55[b]
χ_{gm}	Slope of linear relationship between g_m per leaf area at 25°C and specific leaf nitrogen	mol CO_2 s^{-1} bar^{-1} $mmol^{-1}$ N	5.3E-3[a]	1.6E-2[b]	1.6E-2[b]
N_b	Specific leaf nitrogen below which V_{camx}, J_{max} and V_{pmax} are zero	mmol N m^{-2}	14[c]	14[c]	14[c]
SLN_{ratio_top}	Ratio of the specific leaf nitrogen at the top of the canopy to that of the canopy average	-	1.3[d]	1.3[d]	1.5[d]
C_a	Ambient CO_2 partial pressure	µbar	370[e]	363[f]	363[f]
C_i/C_a	Ratio of intercellular CO2 partial pressure to that of the ambient air	-	0.70[g]	0.45[g]	0.45[g]
w_l	Leaf width	cm	5	15	15
k_u	Canopy wind speed profile coefficient	-	1.5	1.5	1.5

[a], derived from fitting field-observed A/C_i curve reported by Silva-Pérez *et al*. with g_{m25} of 0.55 mol CO_2 m^{-2} s^{-1} bar^{-1} [29] (Fig. S3) and the value of N_b here.

[b], derived from fitting maize A/C_i curve reported by Sharwood *et al.*[30] (Fig. S3) with g_{m25} of 1.2 mol CO_2 m^{-2} s^{-1} bar^{-1} [27] and the value of N_b here.

[c], [24]

[d], derived from the SLN distribution through the canopy in both tall and short sorghums[31]; the value for short sorghum is consistent with that derived from wheat canopy[7].

[e], average of the ambient CO_2 partial pressure in the years when the field experiments in the wheat validation set were conducted: 1998-2007, but the majority are in the earlier range[2].

[f], the ambient CO_2 partial pressure in 1998 when the majority of the field experiments in the sorghum validation set were conducted[1].

[g], typical C_3 value; higher C_4 values are observed in maize[32,33] so 0.45 is used instead of the generally assumed 0.4.

[h], the χ values are reduced to 40% of the tall sorghum (or maize) values to reflect the lower radiation use efficiency observed for short sorghum[1].

Table S7. Input specifications for APSIM wheat and sorghum crop simulations

Description	Units	C_3 wheat	C_4 sorghum
Start date of the multi-year simulation	-	01/01/1900	01/01/1900
End date of the multi-year simulation	-	31/12/2015	31/12/2016
Sowing date	-	15 May	15 October
Sowing density	Plants/m^2	200	6
Sowing depth	mm	30	30
Cultivar (APSIM classification)	-	Hartog	Buster
Row spacing	mm	250	1000 (solid row spacing)
Nitrogen (NO_3) fertiliser at sowing	kg/ha	360	360
Soil type	-	Vertisol (black)	Vertisol (black)
Soil depth	cm	180[a]	180[a]
Soil water at sowing	mm	100	100
Soil NO_3 at sowing	kg/ha	50[b]	50[b]
Soil NH_4 at sowing	kg/ha	5[b]	5[b]

[a] Divided into seven layers having depths of 15, 15, 30, 30, 30, 30 and 30 cm.

[b] Distributed across the seven soil layers using an exponential decay with depth.

Part B: Additional model simulations

Simulated A/C_i curves using the default wheat and sorghum DCaPST parameter sets quantitatively reproduced observations.

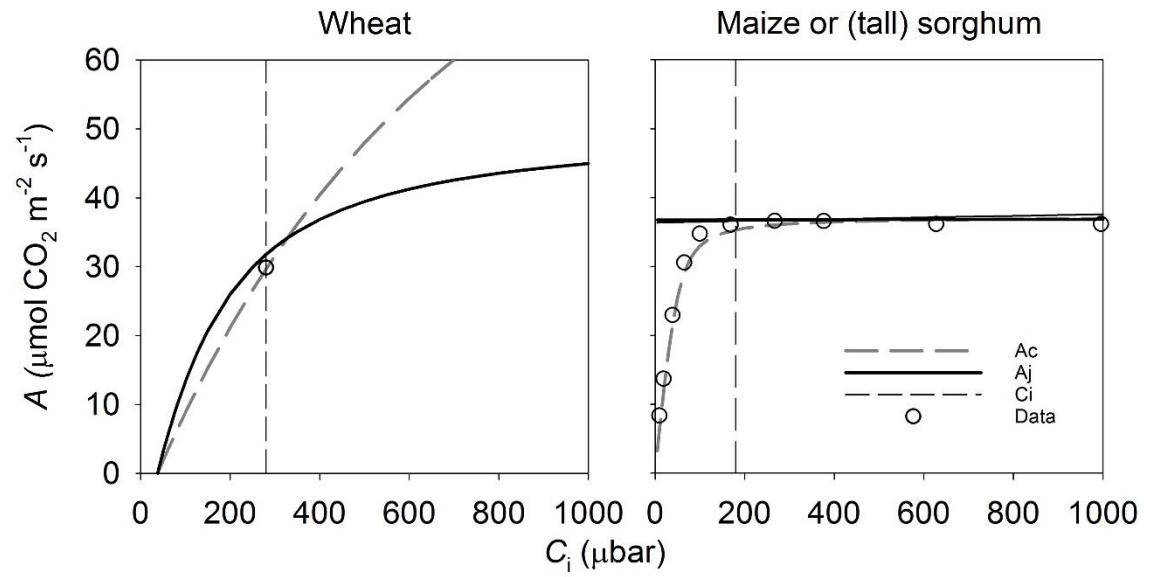

Fig. S3. Simulated and observed CO_2 assimilation rate (A) versus intercellular CO_2 partial pressure (C_i). Observed data are replotted from Silva-Pérez *et al.*[21] for wheat measured in the field, assuming it represents the A_c limited value, and from Sharwood *et al.*[30] for maize. The observed data were obtained at 1800 μmol PAR m^{-2} s^{-1}, which is reflected in the simulation. Specific leaf nitrogen of 1.65 and 1.25 g N m^{-2} are used for wheat and sorghum, respectively, to calculate V_{cmax25}, J_{max25} and V_{pmax25} (equations (S6)–(S9) with SLN_{ratio_top} set to 0 for simulating an isolated leaf) for the simulation. g_{m25} of 0.55 and 1.2 mol CO_2 m^{-2} s^{-1} bar^{-1} are used for wheat and sorghum, respectively. For C_4 photosynthesis, it was assumed that Rubisco, PEP regeneration, and electron transport co-limit CO_2 assimilation at saturating C_i. The fitted V_{cmax} and V_{pmax} were comparable to those obtained by Sharwood et al.[30] The vertical dashed lines indicate C_i at ambient CO_2 of 400 μbar. C_3 and C_4 DCaPST photosynthesis parameterisation are given in Table S6.

Wheat and sorghum biomass for the baseline and photosynthetic manipulation simulations

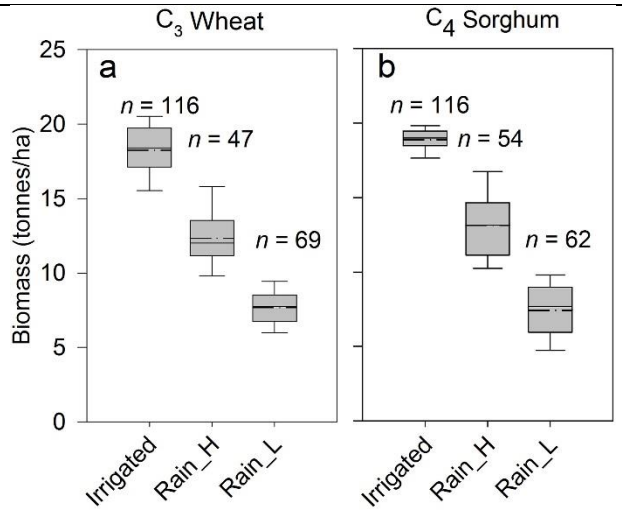

Fig. S4. Baseline simulation of C_3 wheat and C_4 sorghum biomass using 116 years of available weather data. Results for predicted biomass distribution associated with three environment types are shown: Irrigated, non-limiting water supply with full irrigation; Rain_H and Rain_L, rainfed cropping for years with either above or below average yield, respectively. Parameter values for the simulation are given in Tables S6 and S7. Horizontal lines of the boxplots indicate the first quartile, median and third quartile of the yield distribution, whiskers indicate the 10^{th} and 90^{th} percentile, and dash-dot lines are the averages, which are also given in Table S8 (as indicated in the boxplots, *n* = the number of years of simulation in the different environment types).

Simulated crop growth and yield over the crop life cycle for water non-limiting and water-limiting conditions with and without irrigation demonstrating impacts of photosynthetic enhancement on crop water use

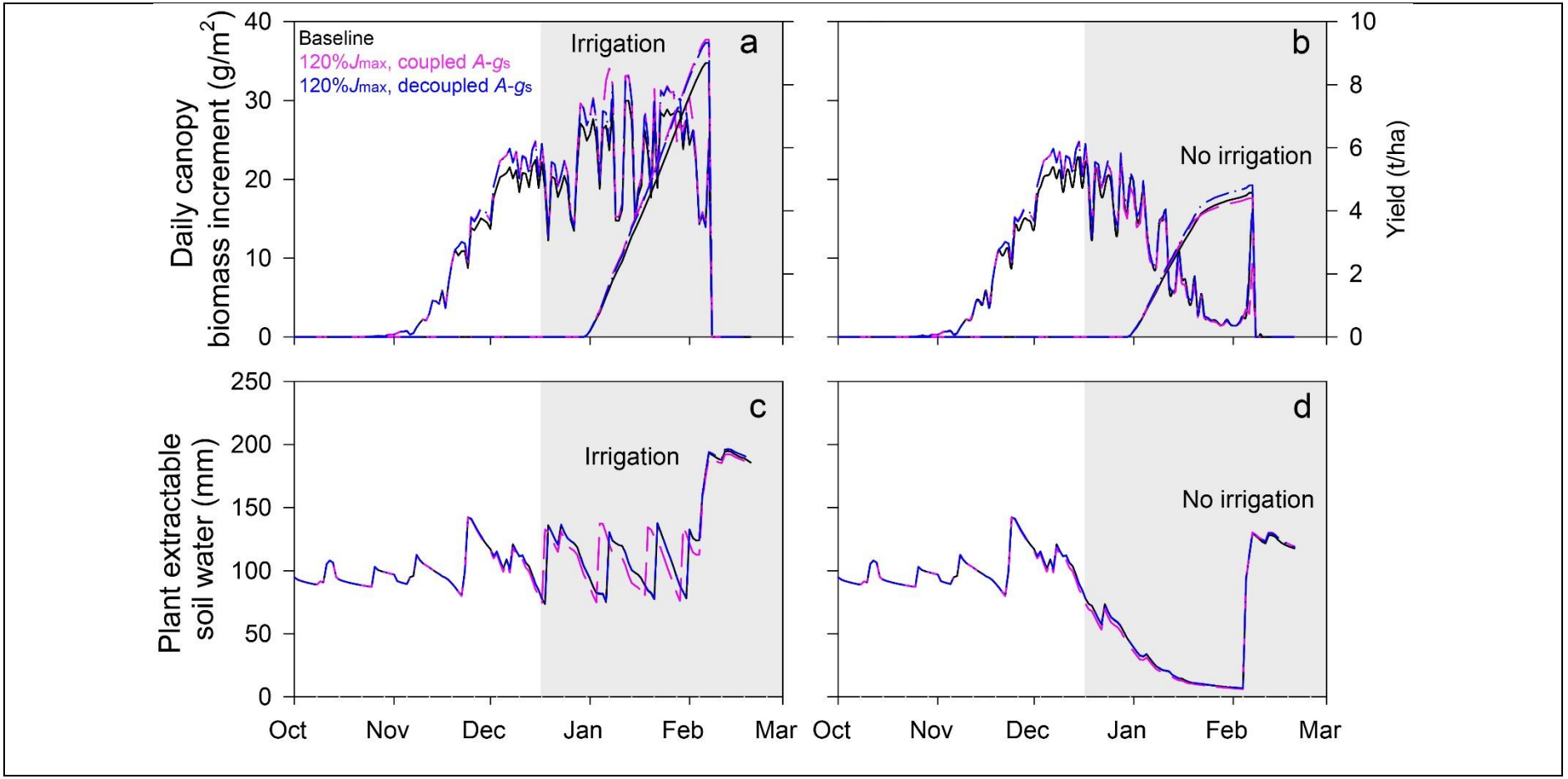

Fig. S5. C_4 sorghum daily crop biomass increment, yield and plant extractable soil water (ESW) content in response to photosynthetic enhancement under water non-limiting (left panels) and water-limiting (right panels) conditions. Black solid curves are simulation for 2007 sowing in the baseline simulation (see main text). The pink and blue dashed curves are 20% enhancement in the maximum electron transport capacity at 25°C (J_{max25}) with A-g_s coupled or decoupled, respectively. Irrigation is added when ESW falls below half its value for a fully wet soil profile. For the 120%J_{max25} scenario, daily crop biomass increment is consistently higher throughout the crop life cycle in the water non-limiting condition for both A-g_s coupled and decoupled situations. In the water-limiting condition, biomass increment is only higher in the first half of the season as ESW becomes depleted after that. However, the A-g_s coupled situation generated a more rapid decline in ESW, which contributed to the lower yield for that scenario. The decoupled A-g_s situation resulted in a similar ESW to the baseline simulation so that the addition biomass increment early in the season contributed to a positive yield impact.

Table S8. Simulated percentage change in average biomass relative to the baseline case with different photosynthetic manipulation targets in different environments. Scenarios also include results for both coupled and decoupled photosynthesis-stomatal conductance (A-g_s) situations. Manipulations include 20% enhancement in the maximum rate of Rubisco activity at 25°C (V_{cmax25}), maximum rate of electron transport at 25°C (J_{max25}), mesophyll conductance at 25°C (g_{m25}), and simultaneous V_{cmax25}-J_{max25}, and V_{cmax25}-J_{max25}-g_{m25} enhancements, while other parameters are kept at their default value (Tables S6 and S7).

	C_3 wheat							C_4 sorghum						
	Biomass (tonnes/ha)	A-g_s coupling	120% V_{cmax25}	120% J_{max25}	120% g_{m25}	120%V_{cmax25} & 120%J_{max25}	120%V_{cmax25} & 120%J_{max25} & 120%g_{m25}	Biomass (tonnes/ha)	A-g_s coupling	120% V_{cmax25}	120% J_{max25}	120% g_{m25}	120%V_{cmax25} & 120%J_{max25}	120%V_{cmax25} & 120%J_{max25} & 120%g_{m25}
Full irrigation	18.2	Yes	0.1%	6.5%	1.3%	10.5%	11.9%	18.9	Yes	0.4%	7.8%	0.0%	9.0%	9.0%
		No	0.1%	5.5%	1.3%	9.3%	10.8%		No	0.4%	7.7%	0.0%	8.9%	8.9%
Rainfed above-average yielding seasons	12.3	Yes	0.0%	5.2%	0.7%	6.8%	7.6%	13.2	Yes	0.5%	3.5%	0.0%	4.6%	4.6%
		No	0.0%	6.2%	0.7%	9.0%	9.9%		No	0.5%	5.3%	0.0%	7.0%	7.1%
Rainfed below-average yielding seasons	7.7	Yes	0.0%	5.3%	0.7%	7.0%	8.0%	7.4	Yes	0.5%	1.4%	0.1%	2.0%	1.7%
		No	0.0%	6.1%	0.7%	9.1%	10.1%		No	0.5%	3.6%	0.1%	5.1%	5.2%

References

1 Hammer, G. L. *et al.* Adapting APSIM to model the physiology and genetics of complex adaptive traits in field crops. *Journal of Experimental Botany* **61**, 2185-2202, doi:10.1093/jxb/erq095 (2010).

2 Brown, H. E. *et al.* Plant modelling framework: software for building and running crop models on the APSIM platform. *Environmental Modelling & Software* **62**, 385-398, doi:10.1016/j.envsoft.2014.09.005 (2014).

3 Sinclair, T. R. & Horie, T. Leaf nitrogen, photosynthesis, and crop radiation use efficiency - a review. *Crop Science* **29**, 90-98 (1989).

4 Robertson, M. J., Fukai, S., Ludlow, M. M. & Hammer, G. L. Water extraction by grain sorghum in a sub-humid environment. I. Analysis of the water extraction pattern. *Field Crops Research* **33**, 81-97, doi:10.1016/0378-4290(93)90095-5 (1993).

5 Ritchie, J. T. Model for predicting evaporation from a row crop with incomplete cover. *Water Resources Research* **8**, 1204-1213, doi:10.1029/WR008i005p01204 (1972).

6 Duncan, W. G., Loomis, R. S., Williams, W. A. & Hanau, R. A model for simulating photosynthesis in plant communities. *Hilgardia* **38**, 181-205 (1967).

7 de Pury, D. G. G. & Farquhar, G. D. Simple scaling of photosynthesis from leaves to canopies without the errors of big-leaf models. *Plant Cell Environ.* **20**, 537-557, doi:10.1111/j.1365-3040.1997.00094.x (1997).

8 Wu, A., Doherty, A., Farquhar, G. D. & Hammer, G. L. Simulating daily field crop canopy photosynthesis: an integrated software package. *Funct. Plant Biol.* **45**, 362-377, doi:10.1071/FP17225 (2018).

9 Boyd, R. A., Gandin, A. & Cousins, A. B. Temperature Responses of C4 Photosynthesis: Biochemical Analysis of Rubisco, Phosphoenolpyruvate Carboxylase, and Carbonic Anhydrase in Setaria viridis. *Plant Physiol.* **169**, 1850-1861, doi:10.1104/pp.15.00586 (2015).

10 Wang, E. *et al.* The uncertainty of crop yield projections is reduced by improved temperature response functions. *Nature Plants* **3**, 17102, doi:10.1038/nplants.2017.102 (2017).

11 Flexas, J., Ribas-Carbo, M., Diaz-Espejo, A., Galmes, J. & Medrano, H. Mesophyll conductance to CO2: current knowledge and future prospects. *Plant Cell Environ.* **31**, 602-621, doi:10.1111/j.1365-3040.2007.01757.x (2008).

12 von Caemmerer, S. *Biochemical models of leaf photosynthesis. Vol. 2*. (CSIRO Publishing, 2000).

13 von Caemmerer, S. & Farquhar, G. D. Some relationships between the biochemistry of photosynthesis and the gas exchange of leaves. *Planta* **153**, 376-387 (1981).

14 Goudriaan, J. & van Laar, H. H. *Modelling Potential Crop Growth Processes : Textbook with Exercises*. (Kluwer Academic Publishers, 1994).

15 McPherson, H. & Slatyer, R. Mechanisms Regulating Photosynthesis in Pennisetum Typhoides. *Aust. J. Biol. Sci.* **26**, 329-340, doi:10.1071/BI9730329 (1973).

16 Leuning, R., Kelliher, F. M., De Pury, D. G. G. & Schulze, E. D. Leaf nitrogen, photosynthesis, conductance and transpiration: scaling from leaves to canopies. *Plant Cell Environ.* **18**, 1183-1200, doi:10.1111/j.1365-3040.1995.tb00628.x (1995).

17 Yin, X. & van Laar, H. H. *Crop Systems Dynamics: An Ecophysiological Simulation Model for Genotype-By-Environment Interactions*. (Wageningen Academic Publishers, 2005).

18 Farquhar, G. D. & Wong, S. C. An empirical-model of stomatal conductance. *Aust. J. Plant Physiol.* **11**, 191-209 (1984).

19 Wong, S. C., Cowan, I. R. & Farquhar, G. D. Stomatal conductance correlates with photosynthetic capacity. *Nature* **282**, 424-426 (1979).
20 Monteith, J. L. & Unsworth, M. H. *Principles of Environmental Physics: Plants, Animals, and the Atmosphere, 4th Edition*. (2013).
21 Silva-Pérez, V., Furbank, R. T., Condon, A. G. & Evans, J. R. Biochemical model of C3 photosynthesis applied to wheat at different temperatures. *Plant Cell Environ.* **40**, 1552-1564, doi:10.1111/pce.12953 (2017).
22 Bernacchi, C. J., Singsaas, E. L., Pimentel, C., Portis Jr, A. R. & Long, S. P. Improved temperature response functions for models of Rubisco-limited photosynthesis. *Plant Cell Environ.* **24**, 253-259, doi:10.1111/j.1365-3040.2001.00668.x (2001).
23 Bernacchi, C. J., Portis, A. R., Nakano, H., von Caemmerer, S. & Long, S. P. Temperature response of mesophyll conductance. Implications for the determination of Rubisco enzyme kinetics and for limitations to photosynthesis in vivo. *Plant Physiol.* **130**, 1992-1998, doi:10.1104/pp.008250 (2002).
24 Braune, H., Mueller, J. & Diepenbrock, W. Integrating effects of leaf nitrogen, age, rank, and growth temperature into the photosynthesis-stomatal conductance model LEAFC3-N parameterised for barley (Hordeum vulgare L.). *Ecol. Modell.* **220**, 1599-1612, doi:10.1016/j.ecolmodel.2009.03.027 (2009).
25 Massad, R.-S., Tuzet, A. & Bethenod, O. The effect of temperature on C4-type leaf photosynthesis parameters. *Plant Cell Environ.* **30**, 1191-1204, doi:10.1111/j.1365-3040.2007.01691.x (2007).
26 von Caemmerer, S. & Evans, J. R. Temperature responses of mesophyll conductance differ greatly between species. *Plant Cell Environ.* **38**, 629-637, doi:10.1111/pce.12449 (2015).
27 Ubierna, N., Gandin, A., Boyd, R. A. & Cousins, A. B. Temperature response of mesophyll conductance in three C4 species calculated with two methods: 18O discrimination and in vitro Vpmax. *New Phytologist* **214**, 66-80, doi:10.1111/nph.14359 (2017).
28 McVicar, T. R. *et al.* Wind speed climatology and trends for Australia, 1975–2006: Capturing the stilling phenomenon and comparison with near-surface reanalysis output. *Geophys. Res. Lett.* **35**, doi:10.1029/2008GL035627 (2008).
29 Silva-Perez, V. *et al.* Hyperspectral reflectance as a tool to measure biochemical and physiological traits in wheat. *Journal of Experimental Botany* **69**, 483-496, doi:10.1093/jxb/erx421 (2018).
30 Sharwood, R. E., Sonawane, B. V. & Ghannoum, O. Photosynthetic flexibility in maize exposed to salinity and shade. *Journal of Experimental Botany* **65**, 3715-3724, doi:10.1093/jxb/eru130 (2014).
31 van Oosterom, E. J., Borrell, A. K., Chapman, S. C., Broad, I. J. & Hammer, G. L. Functional dynamics of the nitrogen balance of sorghum: I. N demand of vegetative plant parts. *Field Crops Research* **115**, 19-28, doi:10.1016/j.fcr.2009.09.018 (2010).
32 Leakey, A. D. B. *et al.* Photosynthesis, Productivity, and Yield of Maize Are Not Affected by Open-Air Elevation of CO(2) Concentration in the Absence of Drought. *Plant Physiol.* **140**, 779-790, doi:10.1104/pp.105.073957 (2006).
33 Pengelly, J. J. L. *et al.* Functional analysis of corn husk photosynthesis. *Plant Physiol.* **156**, 503 (2011).